The Value of Real-Time Adjustable Remedial Action Schemes

Aditya Rangarajan, Line Roald
Department Electrical and Computer Engineering, UW Madison
{arangarajan4, roald}@wisc.edu

***Abstract*—Remedial action schemes (RAS) are often seen as an inexpensive way to relieve contingency-related grid congestion without building new transmission infrastructure. However, RAS settings often remain fixed during real-time operation and do not adapt to variation in operating conditions due to renewable and distributed generation. This lack of adaptability may cause suboptimal settings and possibly insecure operations. To assess the value of allowing RAS settings to vary real time and the benefit of considering multiple load and generation scenarios, we propose a mixed integer optimization framework which identifies optimal RAS actions while incorporating multiple load and renewable energy scenarios. We also propose an iterative algorithm that efficiently solves the optimization problem, leveraging the fact that only a few scenarios and contingencies are binding at optimality. We demonstrate the benefits of (i) updating RAS more frequently and (ii) considering multiple load scenarios by performing case studies on the RTS-GMLC system.**

NOMENCLATURE

A. Abbreviations

RAS	Remedial Action Schemes
OPF	Optimal Power Flow
SCOPF	Security Constrained Optimal power Flow
MILP	Mixed Integer Linear Program

B. Sets and Indices

$i, j \in \mathcal{B}$	Indices/set of nodes
$i \in \mathcal{G}$	Indices/set of generators connected to node i
$ij \in \mathcal{L}$	Indices/set of transmission lines between nodes i and j
$r \in \mathcal{R}$	Indices/set of RAS in the system
$ij \in \mathcal{L}_r$	Indices/set of lines monitored by RAS r
$\mathcal{L}_m$	Set of lines monitored by at least one RAS
$s \in \mathcal{S}$	Indices/set of all load scenarios
$k \in \mathcal{C}$	Indices/set of all $N-1$ contingencies

C. Parameters and Constants

1) Price and Costs:

f_i	Cost function of generator i
γ	Cost of load shedding
β	Cost of RAS action

2) Generator:

$\underline{G}_i, \overline{G}_i$	Lower/upper generation limits of generator i
$g^I_{s,k,i}$	Status of generator i in scenario s after contingency k
K_i	Participation factor of generator i

3) Load:

$D^N_{s,i}$	Pre-contingency load at bus i in scenario s
$D^I_{s,k,i}$	Load at bus i in scenario s after contingency k
$\Delta D^I_{s,k}$	Total load change in the system in scenario s after contingency k

4) Transmission Line:

$\overline{F}_{ij}$	Power flow limit of Line ij
b_{ij}	Admittance of line ij
$l^I_{s,k,ij}$	Status of line ij in scenario s after contingency k

D. Continuous Variables

1) Pre-contingency stage:

$\boldsymbol{F^N_{s,ij}}$	Pre-contingency power flow in line ij, in scenario s
$\boldsymbol{\theta^N_{s,i}}, \boldsymbol{\theta^N_{s,j}}$	Pre-contingency voltage angles at buses i and j in scenario s
$\boldsymbol{G^N_{s,i}}$	Pre-contingency active power output of generator i in scenario s

2) Intermediate stage:

$\boldsymbol{F^I_{s,k,ij}}$	Power flow in line ij immediately after contingency k, in scenario s
$\boldsymbol{\theta^I_{s,k,i}}, \boldsymbol{\theta^I_{s,k,j}}$	Voltage angles at buses i and j in scenario s after contingency k
$\boldsymbol{G^I_{s,k,i}}$	Active power output of generator i in scenario s after contingency k
$\boldsymbol{\Delta G^I_{s,k}}$	Total generation mismatch caused by contingency k in scenario s
$\boldsymbol{\Delta^I_s}$	Total generation mismatch in scenario s caused by the tripping of generators with non-zero participation factors

3) Post-RAS stage:

$\boldsymbol{F^R_{s,k,ij}}$	Power flow in line ij after RAS actions have been implemented in contingency k and scenario s
$\boldsymbol{\theta^R_{s,k,i}}, \boldsymbol{\theta^R_{s,k,j}}$	Voltage angles at buses i and j after RAS actions have been implemented in contingency k and scenario s

The work is supported by the Advanced Grid Modeling Program of the U.S. Department of Energy's Office of Electricity as a part of "Robust Real-Time Control, Monitoring, and Protection of Large-Scale Power Grids in Response to Extreme Events" project.

$G^R_{s,k,i}$ Active power output of generator after RAS actions have been implemented i in contingency k and scenario s

$\Delta G^R_{s,k}$ Total generation mismatch caused by the RAS actions in contingency k and scenario s

Δ^R_s Total generation mismatch in scenario s caused by the RAS tripping generators with non-zero participation factors

$D^R_{s,k,i}$ Load at bus i after the RAS actions have been implemented in contingency k and scenario s

$\Delta D^R_{s,k}$ Total load shed triggered by the RAS actions in contingency k and scenario s

E. Binary Variables

1) RAS triggering conditions:

$z^+_{s,k,ij}$ 1 if line ij is overloaded in the positive direction in contingency k and scenario s, 0 otherwise

$z^-_{s,k,ij}$ 1 if line ij is overloaded in the negative direction in contingency k and scenario s, 0 otherwise

$z_{s,k,ij}$ 1 if line ij is overloaded in either direction in contingency k and scenario s, 0 otherwise

$y_{s,k,r}$ Triggering status of RAS r in contingency k and scenario s (1 if triggered, 0 otherwise)

$\rho_{r,i}$ Optimal actions taken by RAS r (1 if generator i is tripped by RAS r, 0 otherwise)

2) Post-RAS stage:

$\rho^R_{s,k,i}$ Switching status of generator i in contingency k and scenario s after all triggered RAS actions have been implemented

$g^R_{s,k,i}$ Status of generator i after all RAS actions have been implemented (1 if operational, 0 otherwise)

I. Introduction

Due to fundamental changes in the generation sources, increasing peak load, challenges in building new transmission lines and the market-based operation of power systems, the existing electric transmission grid is forced to operate closer to its limits. As a result, system operators are increasingly relying on post-contingency control to avoid post-contingency overloads and maintain secure operation [1], [2]. This has led to the proliferation of remedial action schemes (RAS) ([3], [4]), which detect abnormal system conditions and take fast, predetermined actions in response. Because RAS often reduce post-contingency constraint violations, they are seen as an inexpensive alternative to increase the system's transmission capacity without adding new infrastructure [5], [6].

According to the Western Electricity Coordination Council (WECC), the main RAS parameters are the *arming criteria, initiating/triggering conditions, and the RAS actions* [7]. The arming criteria are critical system conditions for which the RAS should be armed, i.e. ready to take actions when needed. Initiating (or triggering) conditions are contingencies or monitored system conditions that trigger the RAS action if the scheme is already armed. Typical RAS actions include load and generation shedding, transmission line switching, etc. According to [8], for most existing RAS, the arming decision depends on system conditions, while their actions are initiated upon detecting outages and other changes in system topology.

Traditional RAS design procedures are slow and require numerous offline simulations. As a result, RAS settings (i.e., arming criteria, triggering conditions, and RAS actions) often do not change during real-time operations [8]. The slow design procedure along with the use of fixed settings may prevent the RAS from adapting to rapidly evolving grid conditions. While RAS arming/disarming based on real-time system conditions can provide some level of adaptability, the arming criteria are predetermined based on large-scale system studies which includes a given set of assumed system operating conditions. With increased variability due to renewable and distributed generation, the RAS may be subjected to conditions not considered during its design. To mitigate the impacts of this variability, it is important to consider a whole range of load scenarios when designing the RAS and ensure that the RAS is robust for all credible operating conditions. To further improve the performance of the RAS and to prevent misoperations, it would be beneficial to update the RAS settings on an operational time-scale.

Recent research has sought to address the impacts of uncertainty on the ability of preventive and corrective actions to prevent $N-1$ constraint violations. There are many examples in the literature where uncertainty in power injections is modelled when identifying optimal preventive and corrective control actions, see e.g [9], [10], [11], [12], some of which also model situations where the corrective actions fail to operate as intended [13], [14], [15]. However, in the above studies, the corrective control actions are often restricted to generator dispatch and other actions which typically have to be computed and communicated in real-time and are too slow to be classified as RAS.

A realistic RAS includes a local RAS controller that, without further need for communication with a central dispatching entity [16], implements some predetermined actions once a given triggering condition such as a line overload is met, irrespective of the cause. In recent years, there have been efforts to make RAS more adpative [17]. Several RAS implementation that have flexible arming and triggering thresholds (e.g., [18], [19]) or actions (e.g., [20], [21]) have been proposed. In some cases, machine learning has been utilized to adaptively compute RAS parameters. For example, [22] proposed a deep learning based method to identify the optimal load and generation shedding actions, while [23] leverages machine learning to adaptively set the arming criteria of RAS. Although some parameters of these RAS adapt to real-time conditions, most other parameters remain fixed and are determined manually. Another concern with some of these methods is the large amount of historical system data required.

To overcome some of these shortfalls, [24] proposes a sensitivity-based method to generate a set of triggering conditions and RAS actions to address post-contingency line

overloads. However, the proposed method manually identifies suitable RAS actions, which limits the number of contingencies, operating conditions and control actions that can be studied. To further improve the RAS design procedure, [25] developed a method to optimally determine RAS actions that are shared across a large number of contingencies. While [25] demonstrated that optimized RAS is a promising a method for relieving security constraint violations, the results also demonstrated that a RAS scheme is more likely to fail and cause unintended issues if applied in a load and generation scenario that is significantly different than the setting for which it was designed. This highlights the need for real-time adjustible RAS, which we aim to address in this paper.

Specifically, our current paper aims at quantifying the value of adjusting RAS actions in real-time operations, and compare more frequent RAS updates to an approach where the RAS is designed for one or more load and generation scenarios. To achieve this, we make the following contributions. *First*, to address this issue of insecure operations under changing system conditions, we extend the RAS-SCOPF formulation from [25] to incorporate multiple load and renewable energy scenarios. The optimization problem determines a generation dispatch and a set of RAS actions that minimize operational cost across multiple possible operating conditions, and incorporates a model of RAS triggering conditions that give rise to a mixed integer program (MIP). *Second*, because of the binary variables required to model the RAS, incorporating a large number of scenarios is computationally prohibitive. Thus, we propose a solution algorithm that draws inspiration from the iterative decomposition techniques utilized in [14], [26], and [27]. This algorithm leverages the fact that only a few contingencies and load scenarios are binding at optimality [28] and identifies the relevant contingencies and load scenarios using an iterative approach. We find that the algorithm terminates in a few iterations with only a small number of load scenarios and contingencies included, thus greatly simplifying the solution process. *Finally*, we leverage our model to investigate the benefits of (i) updating RAS more frequently in real-time operation and/or (ii) considering multiple load scenarios by performing case studies on the RTS-GMLC system.

The rest of this paper is organized as follows: Section II provides the mathematical description of the problem under consideration, Section III describes the proposed solution algorithm, Section IV presents the results of the case study, and Section V concludes the paper.

II. OPTIMAL DESIGN OF RAS

A. Overview

While RAS may be employed to resolve different kinds of post-contingency problems and may involve different kinds of control actions, we focus on alleviating post-contingency line overloads using generation tripping. Our optimization problem aims to optimally choose a set of RAS actions, i.e. which generators are tripped once the RAS is triggered. RAS actions could be implemented in multiple ways depending on (i) how frequently the system operator updates the RAS actions e.g. based on changing load and generation conditions and (ii) what information is used in deciding whether or not the RAS is triggered. Here, we make the following assumptions:

- **A1** The system operator is able to change the generators tripped by a RAS on an operational time-frame.
- **A2** The RAS is triggered based solely on local measurements of the line loading to enable rapid implementation of the RAS actions after a contingency, without the need for communication with the system operator in real-time.
- **A3** The RAS always works perfectly, i.e. it does not trigger under normal conditions and acts as designed during contingencies.

We note a few important implications of the above assumptions. First, we assume that the RAS is triggered when one of its monitored lines is overloaded, regardless of what caused the line flow to exceed the limit. As a result, the RAS action must be the same regardless of what loading scenario and contingency caused the overload. Second, since we co-design RAS actions of all RAS schemes in response to real-time conditions (Assumption **A1**) and the probability of RAS misoperations or unintended interactions is zero (Assumption **A3**), arming or disarming the RAS does not provide any additional advantages. Therefore, we assume that the RAS is always armed and do not further consider arming as a control variable.

Figure 1 shows a high-level overview of the RAS-SCOPF optimization problem, where we minimize operational cost across multiple loading scenarios (represented as grey boxes). For each loading scenario, we model the operation of the power system in several stages:

(1) *Pre-contingency operation* (highlighted in green) describes the normal operation of the power system for a given load scenario, before any contingency occurs.
(2) *Intermediate operation* (highlighted in red) describes the operation of the power system immediately after a contingency, before any RAS action has been implemented. This stage also includes constraints that model whether or not the RAS are triggered.
(3) *Post-RAS operation* (highlighted in blue) describes the operation of the power system after all the RAS actions have been implemented.

In the following section, we describe the detailed mathematical model of our RAS-SCOPF problem.

B. Formulation of the RAS-SCOPF

We consider a power system where the sets $\mathcal{G}, \mathcal{B}$ and $\mathcal{L}$ represent the generators, buses and lines in the system, and $|\cdot|$ represents the number of elements in each of these sets. $\mathcal{R}$ is the set of all RAS present in the system and for every RAS $r \in \mathcal{R}$, $\mathcal{L}_r$ is the set of lines monitored by that RAS. RAS r is triggered by overloads in any one of the monitored lines $\mathcal{L}_r$. Overloads in lines $\mathcal{L}_m \subset \mathcal{L}$, where $\mathcal{L}_m = \bigcup_{r \in \mathcal{R}} \mathcal{L}_r$, trigger at least one RAS in the system. The RAS are designed to be robust against all scenarios $s \in \mathcal{S}$. The set $\mathcal{C}$ represents the sets of all $N-1$ contingencies, caused by the outage of a single

min **Cost of Pre-Contingency Operations, Post-Contingency Load Shed and Post-Contingency RAS Actions across all Loading Scenarios $S_1, \dots, S_N$, Contingencies $C_1, \dots, C_K$ and RAS schemes $R_1, \dots, R_M$**

s. t.

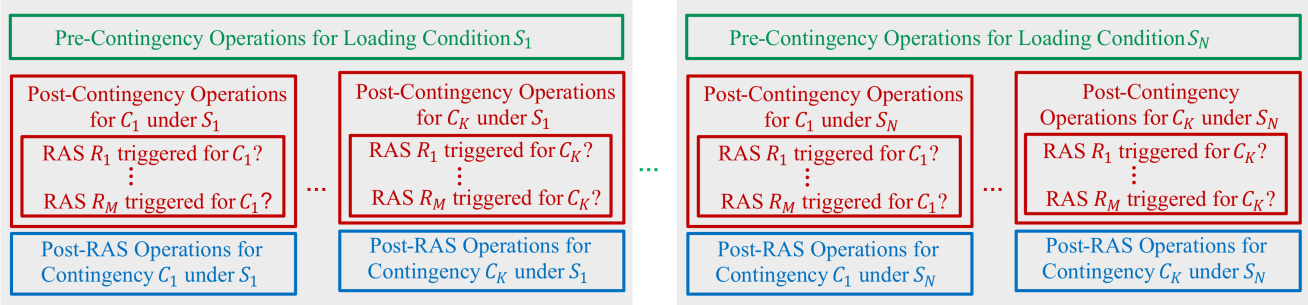

Fig. 1: An overview of the RAS-SCOPF problem.

line or generator in the system. We use **bold** fonts to represent the decision variables, whereas non-bold fonts are used to represent the parameters of the optimization problem. Through out the paper, we use $\boldsymbol{G}$, $\boldsymbol{F}$, $\boldsymbol{\theta}$, $\boldsymbol{D}$ to represent the active power output of each generator, the power flow in each transmission line, the voltage angle and the load at each bus in the system respectively. To simplify the formulation, we assume that there is only one load per bus in the system. Superscripts N, I, and R represent pre-contingency, intermediate, and the post-RAS operations respectively. Subscripts s and k are used to denote the current scenario and contingency respectively. Generator, load, and voltage variables related to individual generator or buses are denoted with subscript i or j, e.g. $\boldsymbol{G^N_{s,i}}$, while lines have double subscripts ij representing either ends of the line, e.g. $\boldsymbol{F^N_{s,ij}}$. The constraints mentioned in this section are enforced for scenarios in $\mathcal{S}$, and except the pre-contingency constraints, are also enforced for all contingencies in $\mathcal{C}$. We do not mention this in every equation due to space constraints. A full nomenclature can be found in the beginning of the paper.

1) Objective: For all the scenarios $s \in \mathcal{S}$, the RAS-SCOPF seeks to minimize the pre-contingency generation costs $f_i(\boldsymbol{G^N_{s,i}})$. The parameter γ, assumed equal for all loads across contingencies and scenarios, represents the cost of load shedding. $D^N_{s,i}$ and $\boldsymbol{D^R_{s,k,i}}$ represent the pre-contingency and the post-RAS load respectively. We also minimize the cost of implementing the RAS actions, represented by the third term in (1). Here, $\boldsymbol{\rho_{r,i}}$ is the switching status of a generator after RAS r has been implemented and β is the cost of generator tripping, which is assumed to be equal for all generators.

$$\min \sum_{s\in\mathcal{S}}\left(\sum_{i\in\mathcal{G}} f_i(\boldsymbol{G^N_{s,i}}) + \sum_{k\in\mathcal{C}(s)}\sum_{i\in\mathcal{B}}\gamma\left(D^N_{s,i} - \boldsymbol{D^R_{s,k,i}}\right)\right) + \sum_{r\in\mathcal{R}}\sum_{i\in\mathcal{G}}\beta\boldsymbol{\rho_{r,i}} \tag{1}$$

2) Pre-contingency Operating constraints: : $(\forall s \in \mathcal{S})$ The following constraints represent the normal operating condition of the system. To simplify the solution, we model the power flows in the system using the DC approximation, represented by (2). Constraint (3) enforces power balance at each node.

$$\boldsymbol{F^N_{s,ij}} = -b_{ij}(\boldsymbol{\theta^N_{s,i}} - \boldsymbol{\theta^N_{s,j}}) \qquad \forall ij \in \mathcal{L} \tag{2}$$

$$\boldsymbol{G^N_{s,i}} - D^N_{s,i} = \sum_{j\in\mathcal{B}} \boldsymbol{F^N_{s,ij}} \qquad \forall i \in \mathcal{B} \tag{3}$$

Constraint (4) models the operational limits of the generators in the system, where $\overline{G}_i$ and $\underline{G}_i$ are the upper and lower generation limits respectively. Constraint (5) limits the the transmission line flows within their thermal limits $\overline{F}_{ij}$.

$$\underline{G}_i \le \boldsymbol{G^N_{s,i}} \le \overline{G}_i \qquad \forall i \in \mathcal{G} \tag{4}$$

$$-\overline{F}_{ij} \le \boldsymbol{F^N_{s,ij}} \le \overline{F}_{ij} \qquad \forall ij \in \mathcal{L} \tag{5}$$

3) Intermediate Operating Constraints: $(\forall s \in \mathcal{S}, k \in \mathcal{C})$ These set of constraints model the operation of the system immediately following a contingency. We make no assumptions on the type of contingency and model the impacts of line, generator, and load outages using the parameters $l^I_{s,k,ij}$, $g^I_{s,k,i}$, and $D^I_{s,k,i}$. For a contingency $k \in \mathcal{C}$, $l^I_{s,k,ij}$ represents the status of each line after the outage, with $l^I_{s,k,ij} = 0$ for the outaged line. Similarly, $g^I_{s,k,i}$ represents the status of generators follwing a generator outage, with $g^I_{s,k,i} = 0$ for the outaged generators (represented by $\mathcal{G}_k$). Finally, $D^I_{s,k,i}$ represents the load at each bus following load outages.

To make up for any power imbalances following a generator or load outage, we assume a distributed slack model and redispatch the system using predetermined participation factors K_i. The loss in generation $\boldsymbol{\Delta G^I_{s,k}}$ following a generator outage is given by (6) and Constraint (7) models the loss in load $\Delta D^I_{s,k}$ due to a load outage.

$$\boldsymbol{\Delta G^I_{s,k}} = \sum_{i\in\mathcal{G}}(1 - g^I_{s,k,i})\boldsymbol{G^N_{s,i}} \tag{6}$$

$$\Delta D^I_{s,k} = \sum_{i\in\mathcal{B}}(D^N_{s,i} - D^I_{s,k,i}) \tag{7}$$

For all active generators (i.e. $\mathcal{G}\backslash\mathcal{G}_k$), the active power output, $\boldsymbol{G^I_{s,k,i}}$, after a contingency, is given by constraints (8) - (9)

$$\boldsymbol{G^I_{s,k,i}} = \boldsymbol{G^N_{s,i}} + K_i(\boldsymbol{\Delta G^I_{s,k}} - \Delta D^I_{s,k} + \boldsymbol{\Delta^I_s}) \tag{8}$$

$$\underline{G}_i \le \boldsymbol{G^I_{s,k,i}} \le \overline{G}_i \tag{9}$$

Where the variable $\boldsymbol{\Delta^I_s}$ represents the power mismatch caused by the outages of generators with non-zero participation fac-

tors. Constraint (10) represents the intermediate power flow $\boldsymbol{F^I_{s,k,ij}}$ in each line, while Constraint (11) enforces nodal power balance.

$$\boldsymbol{F^I_{s,k,ij}} = -l^I_{s,k,ij} b_{ij} (\boldsymbol{\theta^I_{s,k,i}} - \boldsymbol{\theta^I_{s,k,j}}) \qquad \forall ij \in \mathcal{L} \qquad (10)$$

$$\boldsymbol{G^I_{s,k,i}} - D^I_{s,k,i} = \sum_{j \in \mathcal{B}} \boldsymbol{F^I_{s,k,ij}} \qquad \forall i \in \mathcal{B} \qquad (11)$$

For all contingencies $k \in \mathcal{C}$, we relax the line limits of all the monitored lines to observe any overloads in them. For all other lines, Constraint (12) enforces the post-contingency line limits, assuming that lines have the same normal and emergency limits. This constraint, however, can be easily modified to model the temporary overload capacity of transmission lines.

$$-\overline{F}_{ij} \leq \boldsymbol{F^I_{s,k,ij}} \leq \overline{F}_{ij} \qquad \forall ij \in \mathcal{L} \backslash \mathcal{L}_m \qquad (12)$$

4) RAS triggering conditions: $(\forall s \in \mathcal{S}, k \in \mathcal{C})$ For every scenario $s \in \mathcal{S}$, the following constraints evaluate whether the RAS is triggered by overloads in the monitored lines $\mathcal{L}_m$. For every RAS $r \in \mathcal{R}$, Constraints (13) - (17) evaluate if there are overloads in any of its monitored line $\mathcal{L}_r$. Constraints (13) and (14) set the binary variable $\boldsymbol{z^+_{s,k,ij}} = 1$ if the line ij is overloaded in the positive direction. Otherwise, $\boldsymbol{z^+_{s,k,ij}} = 0$.

$$\boldsymbol{F^I_{s,k,ij}} - \overline{F}_{ij} \geq m(1 - \boldsymbol{z^+_{s,k,ij}}) \qquad (13)$$

$$\boldsymbol{F^I_{s,k,ij}} - \overline{F}_{ij} \leq M \boldsymbol{z^+_{s,k,ij}} \qquad (14)$$

Constraints (15) and (16) set the variable $\boldsymbol{z^-_{s,k,ij}} = 1$ if the line ij is overloaded in the negative direction. Else, $\boldsymbol{z^-_{s,k,ij}} = 0$.

$$-\boldsymbol{F^I_{s,k,ij}} - \overline{F}_{ij} \geq m(1 - \boldsymbol{z^-_{s,k,ij}}) \qquad (15)$$

$$-\boldsymbol{F^I_{s,k,ij}} - \overline{F}_{ij} \leq M \boldsymbol{z^-_{s,k,ij}} \qquad (16)$$

If, for every RAS $r \in \mathcal{R}$, a line $ij \in \mathcal{L}_r$ is overloaded in either direction, then constraint (17) sets the variable $\boldsymbol{z_{s,k,ij}} = 1$. Otherwise, $\boldsymbol{z_{s,k,ij}} = 0$.

$$\boldsymbol{z^+_{s,k,ij}} + \boldsymbol{z^-_{s,k,ij}} = \boldsymbol{z_{s,k,ij}} \qquad (17)$$

In the above equations, M and m are big-M constants that represent valid upper and lower bounds on the left-hand sides of the constraints. Constraint (18) evaluates whether RAS r has been triggered or not. Specifically, it sets $\boldsymbol{y_{s,k,r}} = 1$ if the RAS has been triggered, otherwise, $\boldsymbol{y_{s,k,r}} = 0$.

$$\sum_{ij \in \mathcal{L}_r} \boldsymbol{z_{s,k,ij}} \geq \boldsymbol{y_{s,k,r}} \qquad \sum_{ij \in \mathcal{L}_r} \boldsymbol{z_{s,k,ij}} \leq |\mathcal{L}_r| \boldsymbol{y_{s,k,r}} \qquad (18)$$

If RAS r is triggered, then atleast one generator is tripped, i.e,

$$\sum_{i \in \mathcal{G}} \boldsymbol{\rho_{r,i}} \geq 1 \qquad (19)$$

Where, $\boldsymbol{\rho_{r,i}}$ is the switching status of the generator. $\boldsymbol{\rho_{r,i}} = \mathbf{1}$ if generator i is tripped by the RAS. Otherwise $\boldsymbol{\rho_{r,i}} = 0$. Note that the RAS actions $\boldsymbol{\rho_{r,i}}$ are common across scenarios and contingencies, while the RAS triggering conditions (13)-(18) are evaluated for each scenario and contingency.

5) Post-RAS constraints: $(\forall s \in \mathcal{S}, k \in \mathcal{C}(s))$ The following set of constraints model the operation of the system after the RAS has been triggered. Constraints (20)-(22) enforce the action $\boldsymbol{\rho_{r,i}}$ taken by RAS r if it has been triggered, i.e. $\boldsymbol{y_{s,k,r}} = 1$, by contingency $k \in \mathcal{C}$.

$$\boldsymbol{\rho^R_{s,k,r,i}} - \boldsymbol{\rho_{r,i}} \leq (1 - \boldsymbol{y_{s,k,r}}) \qquad (20)$$

$$\boldsymbol{\rho^R_{s,k,r,i}} - \boldsymbol{\rho_{r,i}} \geq (\boldsymbol{y_{s,k,r}} - 1) \qquad (21)$$

$$\boldsymbol{\rho^R_{s,k,r,i}} \leq \boldsymbol{y_{s,k,r}} \quad \boldsymbol{\rho^R_{s,k,r,i}} \geq -(\boldsymbol{y_{s,k,r}}) \qquad (22)$$

Constraints (23) and (24) ensure that all the actions taken by the different RAS in the system are enforced simultaneously.

$$\sum_{r \in \mathcal{R}} \boldsymbol{\rho^R_{s,k,r,i}} \geq \boldsymbol{\rho^R_{s,k,i}} \qquad \sum_{r \in \mathcal{R}} \boldsymbol{\rho^R_{s,k,r,i}} \leq |\mathcal{R}| \boldsymbol{\rho^R_{s,k,i}} \qquad (23)$$

$$\boldsymbol{g^R_{s,k,i}} = g^I_{s,k,i} - \boldsymbol{\rho^R_{s,k,i}} \qquad (24)$$

Where, $\boldsymbol{g^R_{s,k,i}}$ is the generator's operation status after all the RAS actions have been implemented. If the generator continues to operate in the post-RAS stage, then $\boldsymbol{g^R_{s,k,i}} = 1$, otherwise $\boldsymbol{g^R_{s,k,i}} = 0$. In situations where generator shedding is insufficient to prevent overloads in the monitored lines $\mathcal{L}_m$, we also allow load shedding as an emergency action, i.e.,

$$\boldsymbol{D^R_{s,k,i}} \leq D^I_{s,k,i} \qquad \forall i \in \mathcal{B} \qquad (25)$$

The amount of load shed may differ across contingencies k and scenarios s. Constraints (26) - (30) compute the amount of generation and load shed (i.e., $\boldsymbol{\Delta G^R_{s,k}}$ and $\boldsymbol{\Delta D^R_{s,k}}$ respectively) when the RAS actions are implemented.

$$\boldsymbol{\Delta \tilde{G}_{s,k,i}} \leq \overline{G}_i (1 - \boldsymbol{\rho^R_{s,k,i}}) \;\; \boldsymbol{\Delta \tilde{G}_{s,k,i}} \geq \overline{G}_i (\boldsymbol{\rho^R_{s,k,i}} - 1) \qquad (26)$$

$$\boldsymbol{\Delta \tilde{G}_{s,k,i}} - \boldsymbol{G^I_{s,k,i}} \leq \overline{G}_i \boldsymbol{\rho^R_{s,k,i}} \qquad (27)$$

$$\boldsymbol{\Delta \tilde{G}_{s,k,i}} - \boldsymbol{G^I_{s,k,i}} \geq -\overline{G}_i \boldsymbol{\rho^R_{s,k,i}} \qquad (28)$$

$$\boldsymbol{\Delta G^R_{s,k}} = \sum_{i \in \mathcal{G}_k} \boldsymbol{\Delta \tilde{G}_{s,k,i}} \qquad (29)$$

$$\boldsymbol{\Delta D^R_{s,k}} = \sum_{i \in \mathcal{B}} (D^I_{s,k,i} - \boldsymbol{D^R_{s,k,i}}) \qquad (30)$$

Constraints (31)-(32) capture the response of the generators to the generation and load imbalances caused by the RAS actions. The generators respond to these imbalances by adjusting their outputs $\boldsymbol{G^R_{s,k,i}}$ based on their droop factors K_i.

$$\begin{aligned} \boldsymbol{G^R_{s,k,i}} \leq \boldsymbol{G^I_{s,k,i}} &+ K_i (\boldsymbol{\Delta G^R_{s,k}} - \boldsymbol{\Delta D^R_{s,k}} + \Delta^R_s) \\ &+ M(\boldsymbol{g^R_{s,k,i}} - 1) \end{aligned} \qquad (31)$$

$$\begin{aligned} \boldsymbol{G^R_{s,k,i}} \geq \boldsymbol{G^I_{s,k,i}} &+ K_i (\boldsymbol{\Delta G^R_{s,k}} - \boldsymbol{\Delta D^R_{s,k}} + \boldsymbol{\Delta^R_s}) \\ &+ M(\boldsymbol{g^R_{s,k,i}} - 1) \end{aligned} \qquad (32)$$

Constraint (33) restricts the real power outputs of the generators to their limits if the the generator continues to operate after the RAS has been triggered. Otherwise, the output of the generator is set to zero when $\boldsymbol{g^R_{s,k,i}} = 0$.

$$\boldsymbol{g^R_{s,k,i}} \underline{G}_i \leq \boldsymbol{G^R_{s,k,i}} \leq \boldsymbol{g^R_{s,k,i}} \overline{G}_i \qquad \forall i \in \mathcal{G} \qquad (33)$$

Constraints (34) - (36) model the post-RAS operating conditions of the system.

$$\boldsymbol{G^R_{s,k,i}} - \boldsymbol{D^R_{s,k,i}} = \sum_{j \in \mathcal{B}} \boldsymbol{F^R_{s,k,ij}} \qquad \forall i \in \mathcal{B} \qquad (34)$$

$$\boldsymbol{F^R_{s,k,ij}} = -l^I_{s,k,ij} b_{ij} (\boldsymbol{\theta^R_{s,k,i}} - \boldsymbol{\theta^R_{s,k,j}}) \qquad \forall ij \in \mathcal{L}_k \qquad (35)$$

$$-\overline{F}_{ij} \leq \boldsymbol{F^R_{s,k,ij}} \leq \overline{F}_{ij} \qquad \forall ij \in \mathcal{L} \qquad (36)$$

C. Problem variations

To devise effective solution algorithms and benchmark the performance of the RAS-SCOPF, we consider three problem variants, namely a standard OPF, standard SCOPF and a RAS-aware SCOPF.

1) OPF: OPF minimizes pre-contingency generation cost,

$$\min \sum_{i \in \mathcal{G}} f_i(\boldsymbol{G_i^N}) \tag{37}$$

subject only to the pre-contingency constraints (3)-(5).

2) SCOPF: The SCOPF minimizes the pre-contingency generation cost (37) subject to the pre-contingency constraints (3)-(5) and security constraints (8)-(12) to ensure that the system will operate without violations immediately after any contingency has occurred. In the SCOPF, the security constraints are enforced for all lines in the system (i.e. $\mathcal{L}_m = \emptyset$)

3) RAS-aware SCOPF: The RAS-aware SCOPF is a modified version of the preventive SCOPF that minimizes the pre-contingency generation cost (37) subject to the pre-contingency constraints (3) - (5) and post-contingency constraints (9) - (12), except for the post-contingency line limits for the monitored lines $\mathcal{L}_m$. To ensure that the post-RAS generation redispatch is feasible, we include constraints (38)-(40), where $\boldsymbol{r_i}$ is the reserve needed to handle the tripping of generators $\mathcal{G}_{RAS}$ by the RAS.

$$\boldsymbol{\Delta G} = \sum_{i \in \mathcal{G}_{RAS}} \boldsymbol{G_i^N} \tag{38}$$

$$\boldsymbol{r_i} \geq K_i \boldsymbol{\Delta G} \qquad \forall i \in \mathcal{G} \tag{39}$$

$$\boldsymbol{G_i^N} + \boldsymbol{r_i} \leq \overline{\boldsymbol{G}}_{\boldsymbol{i}} \qquad \forall i \in \mathcal{G} \tag{40}$$

III. Solution Algorithm

The full RAS-SCOPF problem described in Section II is a Mixed Integer Linear Program (MILP), with integer variables describing the behaviour of the RAS. Because we are modelling the system operation in three stages and include constraints for each load and contingency scenario, the problem also has a very large number of power flow constraints. The solution times thus can be unacceptably long.

To obtain an optimal solution in reasonable time, we propose an iterative algorithm based on a nested constraint generation approach. In every iteration i, we consider a subset of load scenarios $\mathcal{S}^i \subset \mathcal{S}$. We solve the RAS-SCOPF for the scenarios $\mathcal{S}^i$ while iteratively adding contingency constraints to the problem, with the set $\mathcal{C}_s^i$ representing the considered set of contingencies for scenario s in iteration i. We then run a feasibility check on the remaining scenarios $s \in \mathcal{S} \backslash \mathcal{S}^i$, and add the most violated scenarios to $\mathcal{S}^i$. We then increase the iteration count and resolve the RAS-SCOPF. The algorithm terminates when no more violated scenarios are found, at which point it returns the optimal solution. Note that, as only a few load and contingency scenarios are binding at the optimal solution, the algorithm terminates in only a few iterations. Furthermore, the algorithm provides a lower bound on the optimal objective value in each iteration.

In the following few paragraphs, we describe the algorithm in detail.

TABLE I: Lines Monitored by each RAS scheme

RAS 1	RAS 2	RAS 3
25, 26, 27, 28, 30, 31, 33, 40	119	85

Step 0 Initialization: We initialize the algorithm with a single design scenario in $\mathcal{S}^i$, which we chose to be the peak load scenario. We set the iteration counter to $i = 1$.

Step 1 Solve RAS for load and generation scenarios in $\mathcal{S}_i$: We solve the RAS-SCOPF with scenarios $\mathcal{S}^i$ by iteratively adding violated contingency constraints.

(i) For every scenario $s \in \mathcal{S}^i$, we initialize $\mathcal{C}_s^i = \emptyset$.

(ii) We solve the RAS-SCOPF considering the given scenarios $\mathcal{S}^i$ and contingency sets $\mathcal{C}_s^i$. Let $\boldsymbol{G_s^*}$ be the optimal generation dispatch for scenario $s \in \mathcal{S}^i$and $\boldsymbol{\rho^*}$ the optimal RAS actions shared across scenarios.

(iii) For each scenario $s \in \mathcal{S}^i$, we do the following to identify violated contingencies that were not included in $\mathcal{C}_s^i$.

- **A** Keeping the generation dispatch $\boldsymbol{G_s^*}$ and the RAS actions $\boldsymbol{\rho^*}$ fixed,we solve the intermediate power flow (10)-(11) for all contingencies $k \notin \mathcal{C}_s^i$.
- **B** Given the power flow solutions, we evaluate the RAS triggering conditions (13) - (18). If, for contingency k, a RAS scheme is triggered, then the we implement the actions $\boldsymbol{\rho^*}$ corresponding to the triggered RAS.
- **C** After implementing the RAS actions, we solve the post-RAS power flow and recompute the line flows.

(iv) If none of the contingencies result in constraint violations for any scenario $s \in \mathcal{S}^i$, the RAS-SCOPF solution in step (ii) is feasible for those scenarios. In that case, we terminate *Step 1* and move onto *Step 2*.

(v) If any of the contingencies cause constraint violations, we add two contingencies namely the contingencies that cause the highest constraint violations while triggering or not triggering any RAS, respectively, to $\mathcal{C}_s^i$.

(vi) After expanding the set $\mathcal{C}_s^i$, we return to step (ii).

Step 2 Identify violated scenarios $s \notin \mathcal{S}^i$: Next, we evaluate our solution for scenarios that were not considered in the RAS-SCOPF $s \notin \mathcal{S}^i$. First, we dispatch all the generators in the system by solving the RAS-aware SCOPF, described in II-C, considering one scenario $s \notin \mathcal{S}^i$. Then, following steps **A**-**C**, we evaluate if any contingency results in constraint violations.

Step 3 Termination criterion: If for all scenarios, none of the contingencies result in constraint violations, then the current RAS is optimal and we terminate the algorithm.

Step 4 Adding violated scenarios: If at least one scenario results in post-contingency constraint violations, we include the one with the highest violations in $\mathcal{S}^i$ and return to step 1.

IV. Case Study

The RAS-SCOPF problem and the proposed solution algorithm are implemented in the Julia programming language [29] using JuMP [30] and are solved using the Gurobi v10.0.1 optimizer [31] on a system with a 24 thread Intel(R) Xeon(R) Gold 6248R CPU @ 3.00 GHz. We use the PowerModels.jl package [32] to model the power flow. When solving the RAS-SCOPF, we assume a fixed penalty $\gamma = \$5000$/MW of load

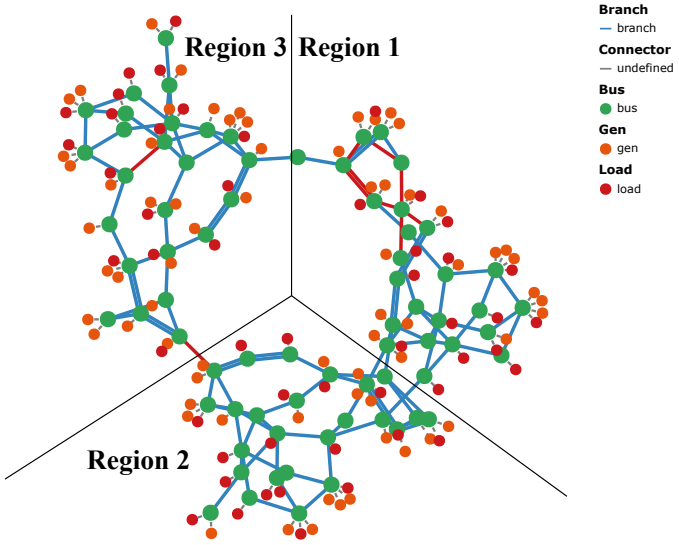

Fig. 2: The RTS-GMLC system (monitored lines highlighted in red)

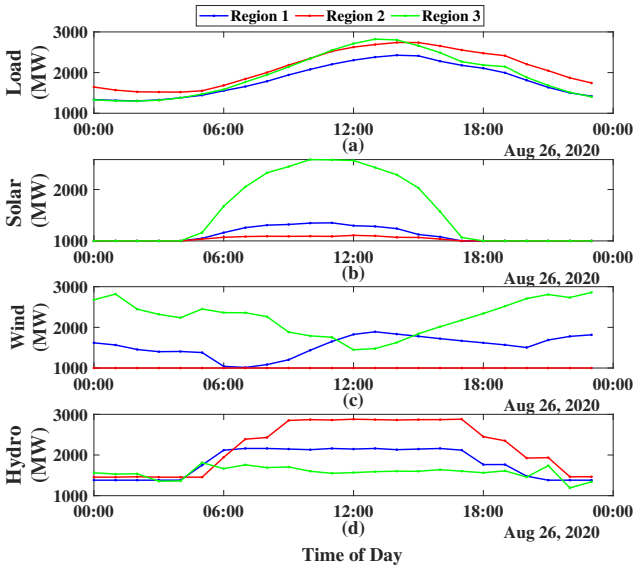

Fig. 3: Region-wise variation in (a) Load and available (b) Solar, (c) Wind, and (d) Hydro generation

shed. When multiple scenarios are considered simultaneously, we use a fixed cost $\beta = \$1000$ for every generator tripped by a RAS. When solving the RAS-SCOPF independently at each scenario, we divide the cost factor β by the total number of scenarios. The Big-M constants are set to $M = -m = 100$.

A. RTS-GMLC system

To demonstrate the advantages of updating RAS actions in real-time as system conditions change, we need a test system with realistic, time-varying load and renewable generation data. We choose to use the RTS-GMLC system [33], which includes year-round load and renewable data[1]. For the case study, we consider 24 hours around the peak load, with one-hour resolution for the load and renewable data. For our contingency set, we consider all non-radial line outages. We

[1]available on https://github.com/GridMod/RTS-GMLC

TABLE II: Solution times when only RAS 1 is considered

Scenarios	Proposed Algorithm		RAS-SCOPF
	Solve Time	Iterations	Solve Time
Peak load	26 s	5	15,221 s
Worst case across scenarios	32 s	5	17,836 s
Designed considering all scenarios	497 s	5	—

remove the HVDC lines and the synchronous condensers and reduce the thermal limits of all the lines by 20% to increase congestion, except for lines 53, 54, 91, and 92 where we double the capacity to ensure feasibility in case of outages.

B. RAS Design

The RTS-GMLC system, shown in Fig. 2, comprises three distinct regions. Region-wise variation in load and renewables, shown in Fig. 3, affects which lines in the system are congested. To design the RAS, we solve the OPF and identify lines that are likely to experience post-contingency overloads. Based on this analysis, we define three RAS. The first RAS monitors line 119, which connects regions 2 and 3, and is often at risk of post-contingency overloads when region 3 has excess renewable energy (i.e. in the middle of the day). We include two additional RAS within region 1 and 3, respectively. These monitor lines that in areas with high renewable penetration that are often at risk of overloads. All the monitored lines are listed in Table I and are highlighted in red in Fig. 2.

C. Computational performance

We first compare the computational performance of the proposed algorithm to the case when the RAS-SCOPF is solved directly using Gurobi v10.0.1. Table II lists the solution times when designing a single RAS for different scenarios and when considering multiple scenarios. As we can see, for all cases, the proposed solution algorithm is significantly faster than solving the full RAS-SCOPF. For many scenarios, the number of contingencies that trigger the RAS, and thus, the number of binary variables are very high. Therefore solving the full RAS-SCOPF can result in unacceptably long solution times. On the other hand, the proposed algorithm is able to find the optimal solution in a few iterations, which means that only a few contingencies and scenarios are binding at the optimal solution. By considering only a small subset of all scenarios and contingencies, we can significantly reduce the number of binary variables and improve the solution times.

We observe similar results when co-optimizing multiple RAS. However, note that in this case, when considering all 24 scenarios simultaneously, all scenarios are binding at the optimal solutions. Thus, the proposed algorithm, for designing multiple RAS while considering multiple scenarios, can still take a long time to converge , although it will still be much faster than solving the full RAS-SCOPF.

D. Impact of multiple RAS schemes

In this section, we assess the benefits of having multiple RAS schemes in the network. We solve the RAS-SCOPF independently for each scenario, first with three RAS schemes and

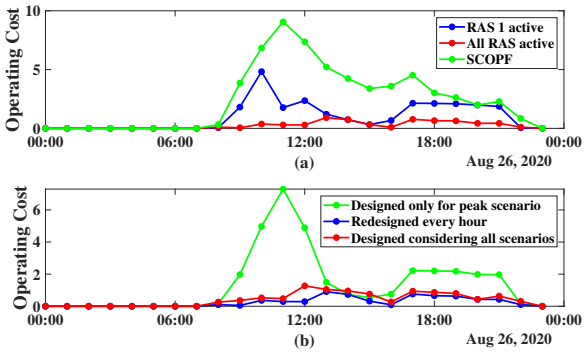

Fig. 4: Plot (a) shows total operating cost obtained by solving the SCOPF and RAS-SCOPF (with single and multiple RAS in the system). Plot (b) shows the total operating cost for different design frequencies and with all RAS active. The operating costs are shown as percent increase compared to the OPF.

then with only RAS 1, and compare the resulting operational cost with the standard OPF and SCOPF (without RAS).

Figure 4(a) shows the operating cost (relative to the OPF) for the SCOPF (in green), the RAS-SCOPF with RAS 1 (in blue) and the RAS-SCOPF with all RAS schemes (in red). First, we observe that the SCOPF always results in the highest generation cost, as it enforces the $N-1$ security constraints without any post-contingency control. The RAS-SCOPF with three active RAS leads to the lowest cost, while the RAS-SCOPF with one active RAS gives intermediate solutions.

Further, due to variations in load and renewable generation, which causes different sets of lines to be congested, the benefits offered by the RAS vary over the course of the day. From 1 am to 8 am, the OPF solution satisfies the $N-1$ security constraints, and we obtain the same generation costs by solving the other formulations. After 5 pm, the generation costs obtained by solving the SCOPF and the RAS-SCOPF with RAS 1 are almost equal, implying that lines other than those monitored by RAS 1 are congested. Installing additional RAS increases flexibility, thus reducing operating costs.

E. Value of real time adjustable RAS

Next, we assess the impact of varying system conditions on the optimal RAS action and the operational cost for the case with three active RAS schemes. Variation in load and renewables can be accounted for either by (i) solving the RAS-SCOPF hourly to redesign the RAS (in which case the RAS actions may vary by hour) or (ii) considering multiple load and generation scenarios when solving the RAS-SCOPF to determine the RAS actions (in which case the RAS actions remain fixed across all hours). These solutions are compared with those when the RAS is designed using only the peak load scenario. When the RAS is designed only for the peak load scenario, we compute the operational cost for other scenarios by fixing the variable $\rho_{r,i}$ and re-solving the RAS-SCOPF. The resulting operational cost and optimal RAS actions are shown in Fig. 4(b) and table III, respectively.

Fig. 4(b) shows that accounting for the variation in system operating conditions by either redesigning the RAS hourly or by considering multiple scenario significantly lowers the operating costs compared to designing only for the peak scenario during many hours per day. Across the full 24h, the total operating cost across 24h is reduced from \$3378318.2 when designing only for the peak load scenario to \$3339586.4 (-1.15%) when redesigned hourly or \$3342605.8 (-1.06%) when designed considering all scenarios. Thus, while redesigning the RAS actions hourly provides the highest amount of flexibility and thus the lowest cost. Almost the same cost reduction can be achieved by accounting for multiple scenarios in the design process. This indicates that it is more important to account for variations in load and renewable generation when choosing the RAS actions than it is to redesign the actions more frequently.

TABLE III: Generators Tripped by each RAS

Time of Day	RAS 1	RAS 2	RAS 3
Designed using the peak load scenario			
All hours	157	—	—
Designed considering all scenarios			
All hours	103, 107, 124, 130, 157	71, 72	156
Redesigned hourly			
8	107	155	—
9	155	155	—
10	9, 57, 71, 74	72, 111, 157	—
11	57, 71, 72	18, 155	—
12	57, 100,157	71, 72	—
13	57, 100,157	111	—
14	103, 107, 157	—	—
15	157	—	—
16-19	157	—	156
20	—	—	156
21	156, 157	—	156
22	157	—	156

To further investigate the differences in solutions, we consider the optimal RAS actions listed in Table III. We first note that when the RAS is designed only for the peak load scenario, only RAS 1 is triggered (i.e., there is no action for RAS 2 and 3). This demonstrates how considering only a single load scenarios fails to take full advantage of the flexibility offered by the RAS. In comparison, designing for multiple scenarios activates RAS 1, 2 and 3 for the full 24h. When the RAS is redesigned hourly, the number of activated RAS schemes and the resulting optimal RAS action vary over time. Importantly, the RAS that is redesigned hourly has fewer generator tripping actions than the RAS designed for multiple scenarios.

Overall, we observe that redesigning the RAS hourly provides the lowest cost and may reduces the number of generators that would be tripped in case of a RAS activation compared to the case designed for multiple scenarios. However, updating RAS actions hourly may be impractical, as it requires communication overheads and possibly long OPF solution times. If this is a concern, designing the RAS for multiple scenarios at once provides similar cost benefits, with the only drawback of a high number of RAS actions.

V. Conclusion

Remedial action schemes (RAS) are an important tool to reduce congestion in power systems operation. However, RAS pose several challenges due to their inability to adapt to changing conditions. To mitigate the impacts of increased variability due to renewable and distributed generation, we proposed

a RAS-SCOPF problem that incorporates multiple load and renewable energy scenario. Also, we devise a nested iterative algorithm to solve the resulting mixed integer problem.

The proposed method is applied to the RTS-GMLC system. *First*, we observe that we can lower the generation costs of the system by including multiple RAS in the network. *Second*, accounting for variation in load and renewable, either by (a) redesigning the RAS every scenario or (b) by incorporating multiple scenarios results in lower operational costs compared to when we design the RAS only for the peak load scenario.

The proposed method provides several opportunities for future work. Firstly, we have assumed that the load and renewable data is fully known, which is not always the case due to measurement and forecast errors. The work in [25] showed that, while the solutions of RAS-SCOPF is secure for small levels of uncertainty, they can fail under high levels of uncertainty. Thus quantifying the impact of uncertainty on the performance of the RAS and formulating the RAS-SCOPF as a stochastic optimization problem will further improve the performance of the RAS. Another important assumption that we have made is that the probability of RAS failure is zero. This is not true in practical scenarios and failures of RAS can have severe consequences. In future, work we would like to model RAS failures and analyse their impact on system reliability. Finally, in the worst case, the proposed algorithm may have to incorporate all the scenarios in solving the RAS-SCOPF, which can still result in unacceptable solution times.The structure of the RAS-SCOPF may allow us to decompose the problem into smaller sub-problems which are easier to solve. We can leverage this fact to further improve the solution speed of RAS-SCOPF.

REFERENCES

[1] F. Capitanescu, J. Martinez Ramos, P. Panciatici, D. Kirschen, A. Marano Marcolini, L. Platbrood, and L. Wehenkel, "State-of-the-art, challenges, and future trends in security constrained optimal power flow," *Elec. Power Sys. Research*, vol. 81, no. 8, pp. 1731–1741, 2011.

[2] P. Panciatici, M. Campi, S. Garatti, S. Low, D. Molzahn, A. Sun, and L. Wehenkel, "Advanced optimization methods for power systems," in *2014 PSCC*, 2014, pp. 1–18.

[3] V. Madani, D. Novosel, S. Horowitz, M. Adamiak, J. Amantegui, D. Karlsson, S. Imai, and A. Apostolov, "IEEE PSRC Report on Global Industry Experiences With System Integrity Protection Schemes (SIPS)," *IEEE Trans on Power Delivery*, vol. 25, no. 4, pp. 2143–2155, 2010.

[4] M. Panteli and P. A. Crossley, "Assessing the risk associated with a high penetration of System Integrity Protection Schemes," in *2012 3rd IEEE PES ISGT Europe*, 2012, pp. 1–7.

[5] J. McCalley, O. Oluwaseyi, V. Krishnan, R. Dai, C. Singh, and K. Jiang, "System protection schemes: limitations, risks, and management," *Final Report to the Power Systems Engineering Research Center*, 2010.

[6] J. Wen, P. Arons, and W.-H. E. Liu, "The role of Remedial Action Schemes in renewable generation integrations," in *2010 ISGT*, pp. 1–6.

[7] W. E. C. C. (WECC), "Remedial action scheme design guide," 2016.

[8] J. O'Brien, R. Huang, E. Barrett, Q. Huang, X. Fan, and R. Diao, "Survey on RAS/SPS modeling practice," 2017.

[9] F. Capitanescu, S. Fliscounakis, P. Panciatici, and L. Wehenkel, "Day-ahead Security Assessment under Uncertainty Relying on the Combination of Preventive and Corrective Controls to Face Worst-Case Scenarios," in *2011 PSCC*. CE - Commission Européenne, 2011.

[10] ——, "Cautious Operation Planning Under Uncertainties," *IEEE Trans. Power Sys.*, vol. 27, no. 4, pp. 1859–1869, 2012.

[11] Á. Porras, L. Roald, J. M. Morales, and S. Pineda, "Integrating Automatic and Manual Reserves in Optimal Power Flow via Chance Constraints," *arXiv preprint arXiv:2303.05412*, 2023.

[12] A. S. Korad and K. W. Hedman, "Robust Corrective Topology Control for System Reliability," *IEEE Trans. Power Sys.*, vol. 28, no. 4, pp. 4042–4051, 2013.

[13] E. Karangelos, P. Panciatici, and L. Wehenkel, "Whither probabilistic security management for real-time operation of power systems?" in *2013 IREP Symposium Bulk Power System Dynamics and Control - IX Optimization, Security and Control of the Emerging Power Grid*, 2013, pp. 1–17.

[14] E. Karangelos and L. Wehenkel, "An Iterative AC-SCOPF Approach Managing the Contingency and Corrective Control Failure Uncertainties With a Probabilistic Guarantee," *IEEE Trans. Power Sys.*, vol. 34, no. 5, pp. 3780–3790, 2019.

[15] ——, "Probabilistic Reliability Management Approach and Criteria for power system real-time operation," in *2016 PSCC*, 2016, pp. 1–9.

[16] S. H. Horowitz, D. Novosel, V. Madani, and M. Adamiak, "System-wide protection," *IEEE Power & Energy Magazine*, vol. 6, no. 5, pp. 34–42, 2008.

[17] M. A. Toro-Mendoza, J. Segundo-Ramírez, A. Esparza-Gurrola, N. Visairo-Cruz, C. A. N. Guitiérrez, and C. Pérez-negrón, "Toward adaptive load shedding remedial action schemes in modern electrical power systems," *IEEE Access*, vol. 11, pp. 111 011–111 033, 2023.

[18] D. S. Baltensperger, "Optimal and adaptive arming of system protection schemes," 2023. [Online]. Available: https://hdl.handle.net/11250/3106065

[19] S. Wang and G. Rodriguez, "Smart ras (remedial action scheme)," in *2010 Innovative Smart Grid Technologies (ISGT)*, 2010, pp. 1–6.

[20] A. Y. Salile, N. Hariyanto, M. Watanabe, and F. S. Rahman, "Adaptive remedial action scheme based on phasor measurement unit," in *2020 International Conference on Smart Energy Systems and Technologies (SEST)*, 2020, pp. 1–6.

[21] S. Yari, H. Khoshkhoo, and N. Hosseinzadeh, "A decentralized remedial action scheme to prevent long-term voltage instability against n-1 and n-2 contingencies," in *2022 IEEE PES 14th Asia-Pacific Power and Energy Engineering Conference (APPEEC)*, 2022, pp. 1–7.

[22] Y. Zhao, S. You, M. Mandich, L. Zhu, C. Zhang, H. Li, Y. Su, C. Zeng, Y. Zhao, Y. Liu, H. Jiang, H. Yuan, Y. Zhang, and J. Tan, "Deep learning-based adaptive remedial action scheme with security margin for renewable-dominated power grids," *Energies*, vol. 14, no. 20, 2021. [Online]. Available: https://www.mdpi.com/1996-1073/14/20/6563

[23] X. Fan, R. Huang, Q. Huang, X. Li, E.L. Barrett, J.G. O'Brien, and Z. Hou, et al, "A Use Case for Transformative Remedial Action Scheme Tool (TRAST): Jim Bridger RAS Evaluation and Analysis," 2019.

[24] H. Li, K. Shetye, T. Overbye, K. Davis, and S. Hossain-Mckenzie, "Towards the automation of remedial action schemes design," 2021.

[25] A. Rangarajan and L. Roald, "Optimal Design and Cascading Failure Evaluation of Remedial Action Schemes," in *2023 IEEE Belgrade PowerTech*, 2023, pp. 1–7.

[26] F. Capitanescu and L. Wehenkel, "A New Iterative Approach to the Corrective Security-Constrained Optimal Power Flow Problem," *IEEE Trans. Power Sys.*, vol. 23, no. 4, pp. 1533–1541, 2008.

[27] L. Roald, S. Misra, T. Krause, and G. Andersson, "Corrective Control to Handle Forecast Uncertainty: A Chance Constrained Optimal Power Flow," *IEEE Trans. Power Sys.*, vol. 32, no. 2, pp. 1626–1637, 2017.

[28] L. A. Roald, D. Pozo, A. Papavasiliou, D. K. Molzahn, J. Kazempour, and A. Conejo, "Power systems optimization under uncertainty: A review of methods and applications," *Elec. Power Sys. Research*, vol. 214, p. 108725, 2023.

[29] J. Bezanson, A. Edelman, S. Karpinski, and V. B. Shah, "Julia: A fresh approach to numerical computing," *SIAM Review*, vol. 59, no. 1, pp. 65–98, 2017.

[30] I. Dunning, J. Huchette, and M. Lubin, "JuMP: A Modeling Language for Mathematical Optimization," *SIAM Review*, vol. 59, no. 2, pp. 295–320, 2017.

[31] Gurobi Optimization, LLC, "Gurobi Optimizer Reference Manual," 2023. [Online]. Available: https://www.gurobi.com

[32] C. Coffrin, R. Bent, K. Sundar, Y. Ng, and M. Lubin, "PowerModels.jl: An Open-Source Framework for Exploring Power Flow Formulations," in *2018 PSCC*, June 2018, pp. 1–8.

[33] C. Barrows, A. Bloom, A. Ehlen, J. Ikäheimo, J. Jorgenson, D. Krishnamurthy, J. Lau, B. McBennett, M. O'Connell, E. Preston, A. Staid, G. Stephen, and J.-P. Watson, "The IEEE Reliability Test System: A Proposed 2019 Update," *IEEE Trans. Power Sys.*, vol. 35, no. 1, pp. 119–127, 2020.